

# Chirality influence on the aggregation

of methyl mandelate

## Supplementary Information

M. Albrecht, A. Borba, K. Le Barbu-Debus, B. Dittrich,  
R. Fausto, S. Grimme, A. Mahjoub, M. Nedić, U. Schmitt,  
L. Schrader, M. A. Suhm\*, A. Zehnacker-Rentien\*, J. Zischang

April 15, 2010

---

\*corresponding authors: msuhm@gwdg.de, anne.zehnacker-rentien@u-psud.fr

Jet FTIR	IR/UV
$\tilde{\nu}(\text{C}-\text{H})$	$\tilde{\nu}(\text{C}-\text{H})$
3101	3104
3076	3080
3043	3045
3009	3009
2964	2963
2904	2900

Table S 1: Experimental band positions of the C–H stretching vibrations in the jet FTIR spectra and in the IR/UV spectra of methyl mandelate obtained with the OPO laser.

	$\Delta E_e$	$\Delta E_0$	$\omega(\text{OH})$	$I$	$\omega(\text{CO})$	$I$
	$\text{kJ mol}^{-1}$	$\text{kJ mol}^{-1}$	$\text{cm}^{-1}$	$\text{km mol}^{-1}$	$\text{cm}^{-1}$	$\text{km mol}^{-1}$
<b>B3LYP/6-31+G*</b>						
SsC			3647	97	1781	250
GskC	8.9	9.3	3731	50	1806	210
<b>MP2/6-31+G*</b>						
SsC			3645	97	1773	208
GskC	7.7	8.3	3713	56	1792	174

Table S 2: Energy difference with ( $\Delta E_0$ ) and without ( $\Delta E_e$ ) zero point correction between the two most stable methyl mandelate monomers and calculated wavenumbers  $\omega$  and band strengths  $I$  for the OH and carbonyl (CO) stretching vibrations.

B3LYP/ 6-31+G*	$D_e$ kJ mol <sup>-1</sup>	$D_0$ kJ mol <sup>-1</sup>	$\omega(\text{OH})$ cm <sup>-1</sup>	$I$ km mol <sup>-1</sup>	$\omega(\text{CO})$ cm <sup>-1</sup>	$I$ km mol <sup>-1</sup>
Hom8a	24.8	19.1	3653	642	1777	209
			3643	260	1776	591
Hom8b	24.5	19.1	3647	922	1775	816
			3641	7	1776	2
<b>Hom8c</b>	<b>28.7</b>	<b>23.4</b>	3593	1639	1770	815
			3575	94	1769	64
Hom4	23.7	18.8	3620	109	1789	342
			3552	642	1777	222
Hom44a	5.2	3.5	3658	79	1786	278
			3653	80	1775	177
Hom44b	10.3	7.9	3639	113	1777	160
			3634	96	1777	342
Hom5a	20.5	15.5	3606	289	1796	160
			3513	634	1789	347
Hom5b	23.6	18.6	3610	345	1797	182
			3566	405	1780	347
<b>Het8a</b>	<b>26.9</b>	<b>21.2</b>	3628	975	1779	779
			3616	0	1776	0
Het8b	24.0	18.6	3619	997	1776	403
			3590	361	1772	483
Het4	12.9	8.4	3665	74	1797	282
			3628	325	1762	338
Het44	8.8	6.8	3661	85	1777	237
			3643	88	1773	257
Het5	24.3	19.6	3600	289	1794	157
			3531	614	1784	367

Table S 3: B3LYP dissociation energies ( $D_0$  and  $D_e$ ) of the homochiral (Hom) and heterochiral (Het) dimers and calculated wavenumbers  $\omega$  and band strengths  $I$  for the OH and carbonyl (CO) stretching vibrations. The most stable (bold face) structure predictions are qualitatively wrong, maximizing the phenyl ring distances (see also Fig. S4).

	$d_{\text{intra}1}$	$d_{\text{intra}2}$	$d_{\text{inter}1}$	$d_{\text{inter}2}$	$R_{\Phi\Phi}(\text{MP2})$	$R_{\Phi\Phi}(\text{B3LYP})$
<b>MP2/6-31+G*</b>						
Hom8a	2.36	2.68	2.05	1.89	4.9	6.3
Hom8b	2.39	2.39	1.97	1.97	3.7	7.1
Hom8c	2.87	2.87	2.00	2.00	9.7	9.7
Hom4	<b>2.02</b>	2.66	—	1.84	3.8	6.8
Hom44a	<b>2.08</b>	<b>2.10</b>	—	—	4.7	6.4
Hom5b	2.42	2.59	1.99	1.89	7.1	8.1
<b>B97-D/def2-TZVP</b>						
Hom8a	2.45	2.68	2.20	1.93		
Hom8b	2.53	2.53	1.99	1.99		
Hom4	<b>2.08</b>	2.62	—	1.87		
Hom44a	<b>2.13</b>	<b>2.34</b>	—	—		
Hom5a	<b>2.22</b>	2.63	2.10	1.86		
Hom5b	2.50	2.60	2.00	1.89		
<b>MP2/6-31+G*</b>						
Het8a	2.93	2.93	1.86	1.86	7.8	8.4
Het8b	2.70	2.77	1.86	1.86	8.0	9.3
Het4	<b>2.13</b>	2.44	—	1.93	4.7	5.6
Het44a	<b>2.04</b>	2.38	—	—	4.7	5.8
Het5	2.28	2.57	2.07	1.85	3.7	7.4
<b>B97-D/def2-TZVP</b>						
Het8a	2.93	2.93	1.88	1.88		
Het8b	2.77	2.80	1.86	1.96		
Het4	2.41	2.52	—	1.97		
Het44a	<b>2.10</b>	2.50	—	—		
Het5	2.49	2.64	2.00	1.88		

Table S 4: Intra- and intermolecular H···O distances (in Å) in the homo- and heterochiral dimers. Bold numbers highlight intramolecular hydrogen bonds shorter than 2.2 Å (MP2) or 2.4 Å (B97-D). The unperturbed monomer hydrogen bond has an H···O distance of 2.07 Å (MP2) and 2.16 Å (B97-D).  $R_{\Phi\Phi}$  denotes the distance between phenyl ring centers at MP2/6-31+G\* and B3LYP/6-31+G\* level.

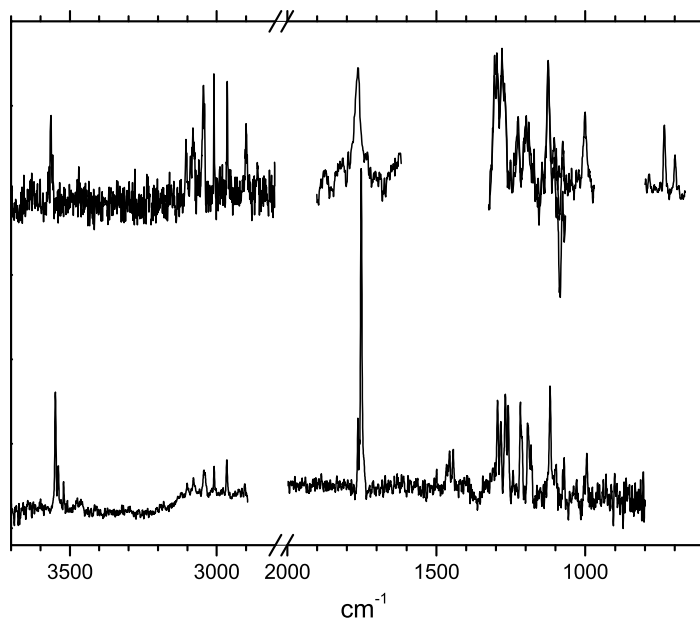


Figure S 1: Experimental IR spectra of methyl mandelate monomer obtained with the FEL at CLIO in the region below  $1800\text{ cm}^{-1}$  and with the OPO laser in the CH/OH stretching region (upper traces, not normalized for laser intensity) in comparison to the FTIR spectra of enantiopure methyl mandelate in the same regions (lower traces). The FTIR spectra (near infrared scaled by 2 because of lower concentration) contain clusters whereas the laser spectra do not. The OH/CH intensity ratio in the FTIR spectra matches the quantum chemical predictions (K. Le Barbu-Debus et al., *J. Phys. Chem. A*, 112:9731–9741, 2008).

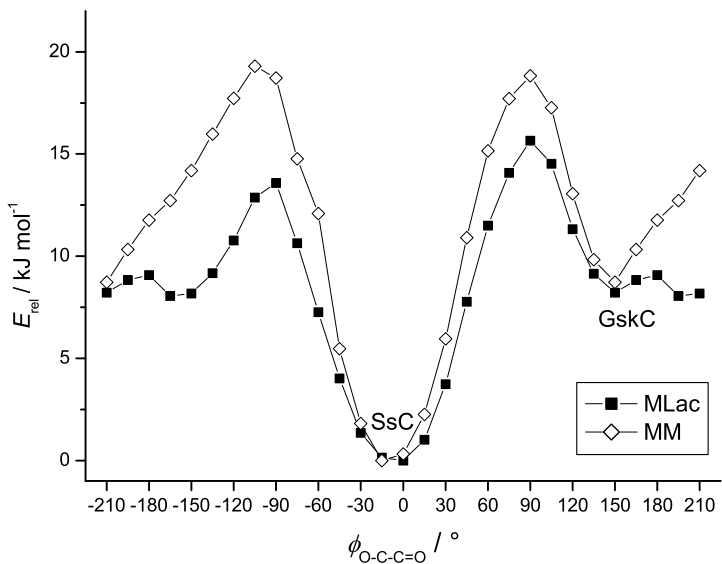


Figure S 2: Relaxed scan (B3LYP/6-31+G\*) of HO-C-C=O torsional angle  $\phi_{\text{O}-\text{C}-\text{C}=\text{O}}$  in methyl mandelate (MM, white diamonds) and methyl lactate (MLac, black squares), showing the deep SsC valley around  $0^\circ$  and secondary ester OR coordinating structures. The zero of the energy scale is taken at the global energy minimum. At this level, the barrier for GskC isomerization is  $19 \text{ kJ mol}^{-1}$  for MM and  $16 \text{ kJ mol}^{-1}$  for MLac ( $14 \text{ kJ mol}^{-1}$  if one accepts the reverse change in torsional angle).

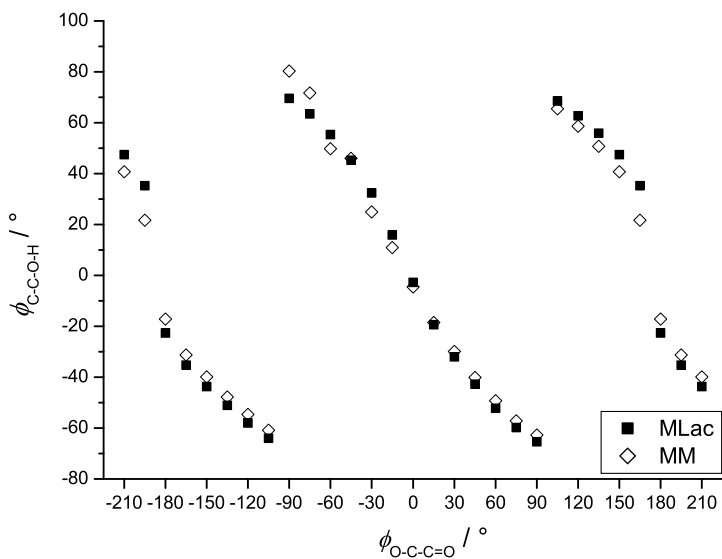


Figure S 3: Change of the C-C-O-H torsional angle of the hydrogen bonded OH-group with the HO-C-C=O torsional angle  $\phi_{O-C-C=O}$  in methyl mandelate (white diamonds) and methyl lactate (black squares). The angles correspond to the most stable structures of the relaxed scan (B3LYP/6-31+G\*). One can see that the OH $\cdots$ O=C hydrogen bond follows the ester distortion for a wide range of angles, before it switches to an OH $\cdots$ OR ester bond.

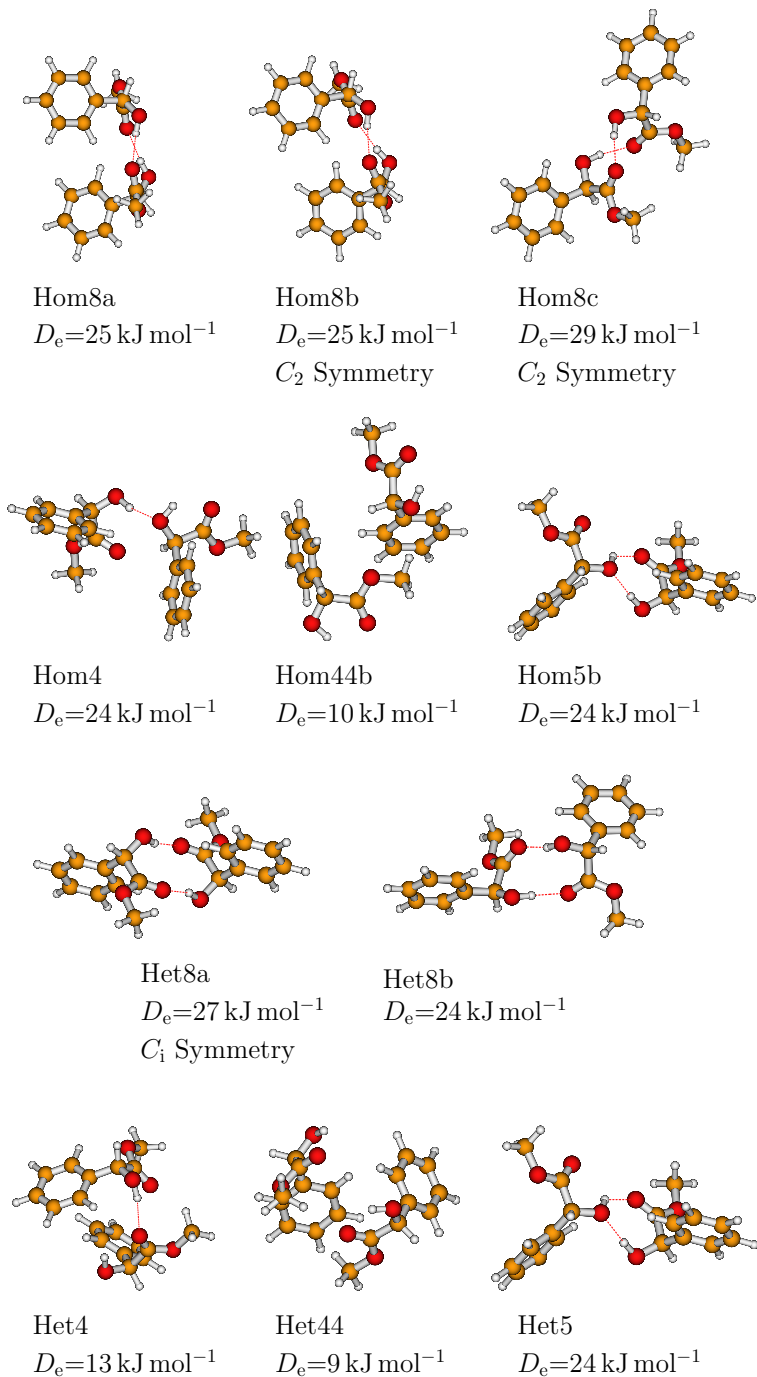


Figure S 4: Homo- (Hom) and heterochiral (Het) MM dimer structures optimized at the B3LYP/6-31+G\* level and their electronic dissociation energies  $D_e$ . The structures differ in the number of heavy atoms involved in the hydrogen bonded ring (8/5/4) and in the axial chirality around the  $C_2$  axis (Hom8b and Hom8c).

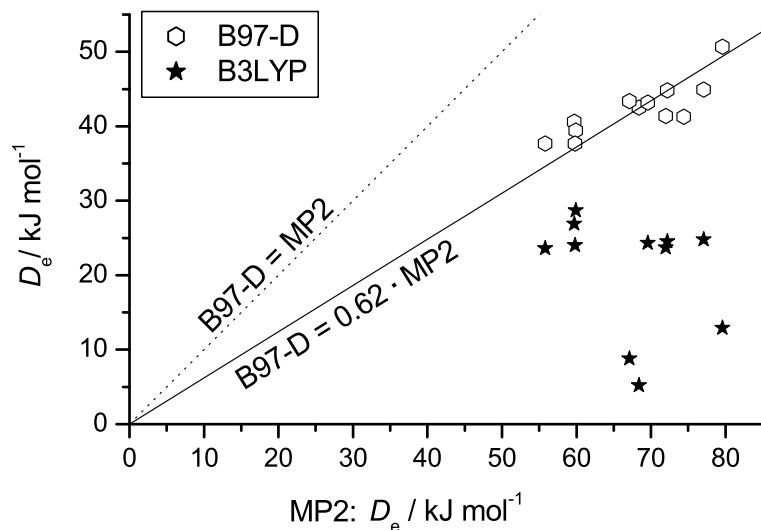


Figure S 5: Dissociation energies  $D_e$  of the dimers without zero-point energy correction at B3LYP/6-31+G\* and B97-D/def2-TZVP level plotted against the corresponding energy at MP2/6-31+G\* level. It is seen that the B3LYP levels fails to capture the relevant dispersion effects whereas the dispersion overestimate of the MP2 level appears to be systematic relative to DFT-D.

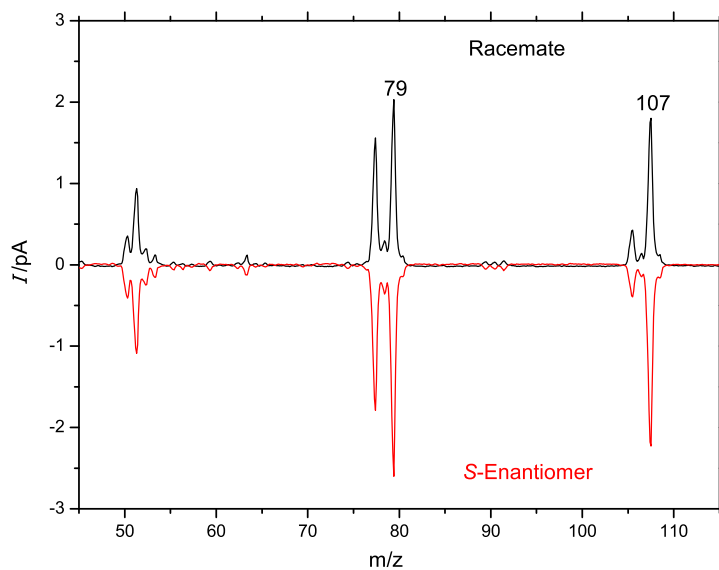


Figure S 6: Mass spectra (ion current  $I/\text{pA}$ ) of racemic and enantiopure methyl mandelate recorded under identical evaporation conditions ( $293.0 \pm 0.5 \text{ K}$ ), reflecting a higher volatility of the enantiopure compound.